

# Alternate Pacing of Border-Collision Period-Doubling Bifurcations

Xiaopeng Zhao<sup>1\*</sup> and David G. Schaeffer<sup>2</sup>

Department of <sup>1</sup>Biomedical Engineering and <sup>2</sup>Mathematics  
and Center for Nonlinear and Complex Systems  
Duke University, Durham, North Carolina 27708

## Abstract

Unlike classical bifurcations, border-collision bifurcations occur when, for example, a fixed point of a continuous, piecewise  $\mathcal{C}^1$  map crosses a boundary in state space. Although classical bifurcations have been much studied, border-collision bifurcations are not well understood. This paper considers a particular class of border-collision bifurcations, i.e., border-collision period-doubling bifurcations. We apply a subharmonic perturbation to the bifurcation parameter, which is also known as alternate pacing, and we investigate the response under such pacing near the original bifurcation point. The resulting behavior is characterized quantitatively by a gain, which is the ratio of the response amplitude to the applied perturbation amplitude. The gain in a border-collision period-doubling bifurcation has a qualitatively different dependence on parameters from that of a classical period-doubling bifurcation. Perhaps surprisingly, the differences are more readily apparent if the gain is plotted vs. the perturbation amplitude (with the bifurcation parameter fixed) than if plotted vs. the bifurcation parameter (with the perturbation amplitude fixed). When this observation is exploited, the gain under alternate pacing provides a useful experimental tool to identify a border-collision period-doubling bifurcation.

## 1 Introduction

In contrast with the usual  $\mathcal{C}^1$  context for classical bifurcations [8], the context of border-collision (B/C) bifurcations is continuous, piecewise  $\mathcal{C}^1$  maps [4, 20]. The simplest normal form of a B/C bifurcation, which we derive below, occurs for iteration of a piecewise linear map as follows

$$x_{n+1} = \begin{cases} Ax_n + c\mu, & \text{if } x_n^{(1)} \geq 0 \\ Bx_n + c\mu, & \text{if } x_n^{(1)} \leq 0 \end{cases}, \quad (1)$$

where  $x$  is an  $m$ -dimensional vector,  $A$  and  $B$  are  $m \times m$  constant matrices,  $c$  is a  $m$ -dimensional constant vector, and the scalar  $\mu$  represents a bifurcation parameter. Here, the term *border* refers to  $x^{(1)} = 0$ , where the superscript indicates the first component of  $x$ : i.e., the border is the surface across which derivatives of the mapping jump.

Examples of B/C bifurcations have been observed in various engineering and biological systems [4, 13, 14, 15]. Different phenomena in B/C bifurcations have been classified by a few authors [1, 3, 4, 5, 6, 7, 9]. Border-collision bifurcations may exhibit surprising phenomena such as so-called instant chaos, which is a direct transition from a fixed point to a chaotic attractor [14].

---

\*Corresponding author. Email: xzhao@duke.edu

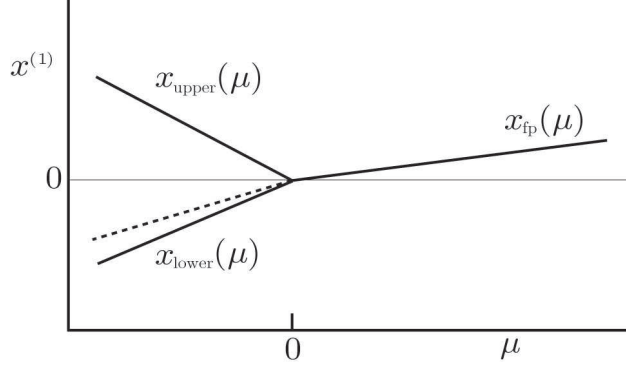


Figure 1: Schematic bifurcation diagram of a border-collision period-doubling bifurcation. Here, the thin horizontal line represents the *border*. Solid lines represent stable solutions whereas the dashed line represents the unstable fixed point.

Alternatively, B/C bifurcations may bear great similarity to their smooth counterparts, such as B/C period-doubling bifurcations [4, 20], which are the main focus of this paper.

Unlike a classical period-doubling bifurcation that occurs when one eigenvalue crosses the unit circle through  $-1$ , eigenvalues are not predictive for the onset of a B/C period-doubling bifurcation. Instead, as indicated in Figure 1, a B/C period-doubling bifurcation occurs when a branch of fixed point *collides* with a border. Despite such intrinsic difference, it may be hard to distinguish between the two bifurcations, especially based on necessarily limited data collected from experiments [2]. This work investigates a possible technique to differentiate between classical and B/C period-doubling bifurcations, inspired by a phenomenon known as prebifurcation amplification previously observed in classical period-doubling bifurcations [17, 18]. The term “prebifurcation amplification” refers to the fact that, near the onset of a classical period-doubling bifurcation, a subharmonic perturbation to the bifurcation parameter leads to amplified disturbances in the system response. In the literature, such subharmonic perturbations are also referred to as *alternate pacing* [2, 12, 19]. The amplification due to alternate pacing of a classical bifurcation has been characterized by a gain relating the disturbances in response to the perturbation amplitude [17, 18, 19]. In this paper, we compute the gain for a B/C period-doubling bifurcation under alternate pacing. Specifically, we find that the gain of a B/C bifurcation, as a function of the bifurcation parameter and the perturbation amplitude, differs significantly from that of a classical bifurcation.

In Section 2, we first investigate the conditions for the existence and stability of a B/C period-doubling bifurcation. Then, the response of a B/C period-doubling bifurcation to alternate pacing is derived in Section 3. Section 4 quantifies the effect of prebifurcation amplification through a gain. Finally, Section 5 provides a concluding discussion.

## 2 Hypotheses and Notation

### 2.1 Normal form of a border-collision bifurcation

We first derive the normal form (1). Consider iteration under a general border-collision (B/C) map

$$z_{n+1} = f(z_n, \nu), \quad (2)$$

where  $z_n \in \mathbb{R}^m$ ,  $\nu$  is a bifurcation parameter, and

$$f(z, \nu) = \begin{cases} f_A(z, \nu), & \text{if } \beta(z, \nu) \geq 0 \\ f_B(z, \nu), & \text{if } \beta(z, \nu) \leq 0 \end{cases}. \quad (3)$$

To have a B/C bifurcation, we impose the following three conditions on the above map.

**Condition 1:** Continuity on the boundary:  $f_A(z, \nu) = f_B(z, \nu)$  whenever  $\beta(z, \nu) = 0$ .

**Condition 2:** For  $\nu = \nu_{\text{bif}}$ , (3) has a fixed point  $z_{\text{bif}}$  on the boundary, i.e.,

$$\beta(z_{\text{bif}}, \nu_{\text{bif}}) = 0 \quad (4)$$

and  $z_{\text{bif}} = f_A(z_{\text{bif}}, \nu_{\text{bif}}) = f_B(z_{\text{bif}}, \nu_{\text{bif}})$ .

**Condition 3:** The boundary is locally nonsingular; in symbols

$$\nabla\beta|_{\text{bif}} \equiv \nabla\beta(z_{\text{bif}}, \nu_{\text{bif}}) \neq 0, \quad (5)$$

where  $\nabla$  indicates the vector of derivatives of  $\beta$  with respect to  $z_1, \dots, z_m$ ; i.e., it does not include the  $\nu$  derivative.

To derive the normal form, choose an invertible matrix  $R$  s.t.

$$R(\nabla\beta|_{\text{bif}}) = e_1, \quad (6)$$

where  $e_1 = (1, 0, \dots, 0)^T$ . Let  $b$  be the vector

$$b = (\partial_\nu\beta|_{\text{bif}}) e_1. \quad (7)$$

Making a change of coordinates

$$x = R(z - z_{\text{bif}}) + (\nu - \nu_{\text{bif}}) b, \quad \mu = \nu - \nu_{\text{bif}} \quad (8)$$

and dropping all higher order terms in (2) yields a map that assumes the form (1), where

$$A = R(Df_A|_{\text{bif}})R^{-1}, \quad B = R(Df_B|_{\text{bif}})R^{-1} \quad (9)$$

$$c = b - Ab - R(\partial_\nu f_A|_{\text{bif}}) = b - Bb - R(\partial_\nu f_B|_{\text{bif}}). \quad (10)$$

Here,  $Df$  denotes the differential of  $f$ , i.e., the  $m \times m$  matrix of partial derivative of  $f$  with respect to  $z_1, \dots, z_m$ . Note that the two expressions of the vector  $c$  are equal due to the continuity of  $f$ . As will be seen later, condition 4 below requires that  $c \neq 0$ .

**Remark:** The continuity condition (#1 above) implies that  $Ax = Bx$  if  $x^{(1)} = 0$ . Thus, only nonzero column of  $B - A$  is the first column.

## 2.2 Conditions for the period-doubling case

For the rest of the paper, we assume map (1) undergoes a B/C period-doubling bifurcation as illustrated in Figure 1. Specifically, we assume that:

**Hypothesis 1:** (a) For  $\mu > 0$ , map (1) has a stable fixed point  $x_{\text{fp}}(\mu)$  in the half space  $\{x^{(1)} > 0\}$ . (b) For  $\mu < 0$ , there exists a fixed point in the half space  $\{x^{(1)} < 0\}$  but it is unstable.

**Hypothesis 2:** For  $\mu < 0$ , (1) has a stable period-two orbit, with one point in  $\{x^{(1)} > 0\}$  and the other in  $\{x^{(1)} < 0\}$ .

Conditions 4-6 below guarantee that (1) possesses this structure. We do *not* assume that the fixed point for  $\mu > 0$  is the only attractor nor do we assume the period-two orbit for  $\mu < 0$  is the only attractor. Indeed, the analysis of Banerjee and Grebogi [1] suggests that, more often than not, there will be additional attractors.

### 2.2.1 Analysis of fixed point solutions

When  $\mu > 0$ , a fixed point of (1) in the half space  $\{x^{(1)} > 0\}$  must satisfy

$$x_{\text{fp}}(\mu) = \mu X_{\text{fp}}, \quad (11)$$

where  $X_{\text{fp}}$  is the constant vector

$$X_{\text{fp}} = (I - A)^{-1} c. \quad (12)$$

By hypothesis 1 (a), we have the following condition.

**Condition 4:** The first component of the vector  $X_{\text{fp}}$  is positive, i.e.,  $X_{\text{fp}}^{(1)} > 0$ , and all eigenvalues of  $A$  are inside the unit circle, i.e.,  $\forall i, |\lambda_i(A)| < 1$ .

When  $\mu < 0$ , the unstable fixed point in  $\{x^{(1)} < 0\}$  is given by

$$x_{\text{unstable}}(\mu) = \mu (I - B)^{-1} c, \quad (13)$$

and by hypothesis 1 (b) we have the following condition.

**Condition 5:** The first component of the vector  $(I - B)^{-1} c$  is positive and at least one eigenvalue of  $B$  satisfies that  $|\lambda_i(B)| > 1$ .

### 2.2.2 Analysis of period-two solutions

When  $\mu < 0$ , let us write  $x_{\text{upper}}(\mu)$ ,  $x_{\text{lower}}(\mu)$  for the stable period-two orbit of (1), where as in Figure 1  $x_{\text{upper}}(\mu)$  is the point in  $\{x^{(1)} > 0\}$ . These points satisfy

$$x_{\text{upper}}(\mu) = B x_{\text{lower}}(\mu) + \mu c, \quad x_{\text{lower}}(\mu) = A x_{\text{upper}}(\mu) + \mu c \quad (14)$$

It follows from the above equations that

$$x_{\text{upper}} = \mu X_{\text{upper}}, \quad x_{\text{lower}} = \mu X_{\text{lower}}, \quad (15)$$

where

$$X_{\text{upper}} = (I - BA)^{-1} (I + B) c, \quad X_{\text{lower}} = (I - AB)^{-1} (I + A) c. \quad (16)$$

For these calculations to be consistent and for the orbit to be stable, we need the following condition.

**Condition 6:**  $X_{\text{upper}}^{(1)} < 0$ ,  $X_{\text{lower}}^{(1)} > 0$ , and  $\forall i, |\lambda_i(AB)| < 1$ . (Note that matrices  $AB$  and  $BA$  have same characteristic polynomials and hence have the same eigenvalues.)

## 3 The response to alternate pacing

Alternate pacing imposes a subharmonic perturbation to the bifurcation parameter  $\mu$ , rendering the map (1) as

$$x_{n+1} = \begin{cases} Ax_n + [\mu + (-1)^n \delta] c, & \text{if } x_n^{(1)} > 0 \\ Bx_n + [\mu + (-1)^n \delta] c, & \text{if } x_n^{(1)} < 0 \end{cases}, \quad (17)$$

For use below, we define

$$d = (I + A)^{-1} c; \quad (18)$$

to avoid a degenerate response to alternate pacing, we impose the following condition.

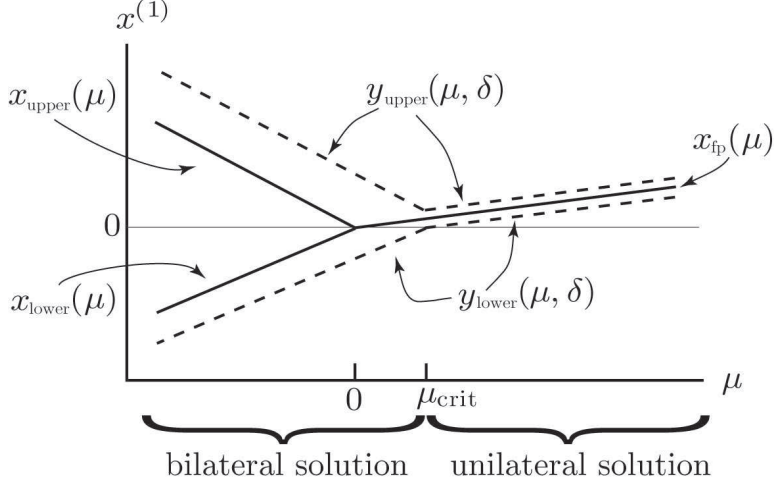


Figure 2: Unilateral and bilateral solutions of alternate pacing (dashed) compared to the solutions when  $\delta = 0$  (solid). The thin horizontal line represents the border.

**Condition 7:** The first component of the vector  $d$  is nonzero, i.e.,  $d^{(1)} \neq 0$ .

We are interested in period-two solutions of (17), whose two points are denoted by  $y_{\text{upper}}(\mu, \delta)$  and  $y_{\text{lower}}(\mu, \delta)$ . As depicted in Figure 2 and will be derived in the following, the character of the period-two solution depends on  $\mu$ . 1.) For  $\mu > \mu_{\text{crit}}(\delta)$ , where  $\mu_{\text{crit}}(\delta)$  is defined in (23) below, the response is a unilateral solution: i.e., both points are above the border, or in symbols  $y_{\text{upper}}^{(1)} > y_{\text{lower}}^{(1)} > 0$ ; and 2.) For  $\mu < \mu_{\text{crit}}(\delta)$ , the response is a bilateral solution: i.e., one point is above and the other is below the border, or in symbols  $y_{\text{upper}}^{(1)} > 0 > y_{\text{lower}}^{(1)}$ .

### 3.1 The unilateral solution

To compute the unilateral solution, we first need to determine whether  $y_{\text{upper}}(\mu, \delta)$  occurs in the iteration for  $n$  even or odd. To this end, we temporarily denote the two points as  $y_{\text{odd}}(\mu, \delta)$  and  $y_{\text{even}}(\mu, \delta)$ . In the unilateral case, i.e.  $y_{\text{odd}}^{(1)}, y_{\text{even}}^{(1)} > 0$ , equation (17) leads to

$$y_{\text{odd}} = A y_{\text{even}} + (\mu + \delta) c, \quad y_{\text{even}} = A y_{\text{odd}} + (\mu - \delta) c. \quad (19)$$

Solving the above equations yields

$$y_{\text{odd}}(\mu, \delta) = x_{\text{fp}}(\mu) + \delta d, \quad y_{\text{even}}(\mu, \delta) = x_{\text{fp}}(\mu) - \delta d, \quad (20)$$

where  $x_{\text{fp}}$  and  $d$  are computed in (11) and (18), respectively. By adopting the sign convention

$$\text{sign } \delta = \text{sign } d^{(1)}, \quad (21)$$

we can arrange that  $y_{\text{upper}}$  and  $y_{\text{lower}}$  correspond to odd- and even-numbered beats, respectively; that is

$$y_{\text{upper}}(\mu, \delta) = x_{\text{fp}}(\mu) + \delta d, \quad y_{\text{lower}}(\mu, \delta) = x_{\text{fp}}(\mu) - \delta d. \quad (22)$$

In the remainder of the paper, we retain the notation  $y_{\text{upper}}$  and  $y_{\text{lower}}$ , assuming the sign convention (21).

The unilateral solution is valid provided  $y_{\text{lower}}^{(1)} \geq 0$ , that is

$$\mu \geq \rho |\delta| \equiv \mu_{\text{crit}}(\delta), \quad (23)$$

where

$$\rho = \frac{|d^{(1)}|}{X_{\text{fp}}^{(1)}} > 0. \quad (24)$$

At the critical value of  $\mu$ , we have

$$y_{\text{upper}}(\mu_{\text{crit}}(\delta), \delta) = x_{\text{fp}}(\mu_{\text{crit}}(\delta)) + \delta d \equiv y_{\text{u-crit}}(\delta) \quad (25)$$

$$y_{\text{lower}}(\mu_{\text{crit}}(\delta), \delta) = x_{\text{fp}}(\mu_{\text{crit}}(\delta)) - \delta d \equiv y_{\text{l-crit}}(\delta). \quad (26)$$

Note that  $y_{\text{u-crit}}^{(1)} > 0$  and  $y_{\text{l-crit}}^{(1)} = 0$ .

### 3.2 The bilateral solution

We now compute the bilateral solution that evolves continuously from the unilateral solution<sup>1</sup> as  $\mu$  crosses  $\mu_{\text{crit}}(\delta)$ . Thus, for  $\mu < \mu_{\text{crit}}(\delta)$ , we look for a period-two orbit of (17) such that

$$y_{\text{upper}}^{(1)}(\mu, \delta) > 0 > y_{\text{lower}}^{(1)}(\mu, \delta), \quad (27)$$

where  $y_{\text{upper}}$  occurs for  $n$  odd. By (17), these satisfy

$$y_{\text{upper}} = B y_{\text{lower}} + (\mu + \delta) c, \quad y_{\text{lower}} = A y_{\text{upper}} + (\mu - \delta) c. \quad (28)$$

Comparing these equations with (14), we see that the solution of (28) may be written as

$$y_{\text{upper}}(\mu, \delta) = x_{\text{upper}}(\mu) + \delta s_{\text{upper}}, \quad y_{\text{lower}}(\mu, \delta) = x_{\text{lower}}(\mu) - \delta s_{\text{lower}}, \quad (29)$$

where  $x_{\text{upper}}$  and  $x_{\text{lower}}$  have been computed in (15), and the  $\mu$ -independent shifts  $s_{\text{upper}}$ ,  $s_{\text{lower}}$  are given by

$$s_{\text{upper}} = (I - BA)^{-1} (I - B) c, \quad s_{\text{lower}} = (I - AB)^{-1} (I - A) c. \quad (30)$$

We now show that this solution is consistent with the assumption (27). We claim that when  $\mu = \mu_{\text{crit}}(\delta)$ , the solution (25,26) of (19) for this value of  $\mu$  also satisfies (28); this claim follows from the observation that, since  $y_{\text{l-crit}}^{(1)} = 0$ , we have  $A y_{\text{l-crit}} = B y_{\text{l-crit}}$ . Using the fact that  $x_{\text{upper}}$  and  $x_{\text{lower}}$  are linear in  $\mu$ , we may rewrite (29) as

$$\begin{aligned} y_{\text{upper}}(\mu, \delta) &= y_{\text{upper}}(\mu_{\text{crit}}(\delta), \delta) + x_{\text{upper}}(\mu) - x_{\text{upper}}(\mu_{\text{crit}}(\delta)) \\ &= y_{\text{u-crit}}(\delta) + (\mu - \mu_{\text{crit}}(\delta)) X_{\text{upper}} \end{aligned} \quad (31)$$

and

$$y_{\text{lower}}(\mu, \delta) = y_{\text{l-crit}}(\delta) + (\mu - \mu_{\text{crit}}(\delta)) X_{\text{lower}}. \quad (32)$$

It now follows from Condition 6 that (27) holds for all  $\mu < \mu_{\text{crit}}(\delta)$ .

---

<sup>1</sup>In the appendix, we show that for  $\mu$  sufficiently large negative there is also a second bilateral solution.

### 3.3 Stability of perturbed iterations

The unperturbed map (1), without alternate pacing as in (17), may suffer a so-called dangerous bifurcation [10] at  $\mu = 0$ . To elaborate: suppose that at some positive value of  $\mu$  the (unperturbed) iteration is locked onto  $x_{\text{fp}}(\mu)$ . If  $\mu$  is decreased quasistatically but remains positive, the solution will follow the stable fixed point  $x_{\text{fp}}(\mu)$ . However, as  $\mu \rightarrow 0$ , the basin of attraction of the fixed point might shrink to nil. In this case, the iteration becomes indeterminate as  $\mu$  crosses 0, i.e., as a result of infinitesimal perturbations, the solution might shift to a different attractor for  $\mu < 0$  rather than to the period-two solution.

One may hope that iterations of (17), i.e., the map under alternate pacing, are better behaved near  $\mu = \mu_{\text{crit}}(\delta)$  when they cross the boundary plane  $\{x^{(1)} = 0\}$ . However, we are unable to guarantee this without imposing an additional hypothesis, as follows.

**Condition 8:** There exists an invertible matrix  $S$  s.t.  $\|S A^2 S^{-1}\| < 1$  and  $\|S A B S^{-1}\| < 1$ . In other words, the eigenvectors for  $A^2$  and  $A B$  are not too different. For example, this condition is satisfied if both  $A^2$  and  $A B$  are both diagonalizable using  $S$ .

In the following lemma, we consider the composition of (17) with itself when  $\mu \approx \mu_{\text{crit}}(\delta)$ , starting with  $n$  even from an  $x$  near the even iterates  $y_{\text{lower}}$  of the period-two orbit, for which we have  $y_{\text{lower}}^{(1)}(\mu, \delta) \approx y_{\text{l-crit}}^{(1)} = 0$ . Thus, both options in (17) must be considered for the first application of (17). However, the image of  $x$  will be close to the odd iterates, for which we have  $y_{\text{upper}}^{(1)}(\mu, \delta) \approx y_{\text{u-crit}}^{(1)} > 0$ . Thus, provided  $\mu$  is sufficiently close to  $\mu_{\text{crit}}(\delta)$  and  $x$  is sufficiently close to  $y_{\text{lower}}^{(1)}(\mu, \delta)$ , only the upper option in (17) will occur in the second application of (17). Thus, if  $\mu$  and  $x$  are so restricted, the composition of (17) with itself is given by

$$F(x) = \begin{cases} A[Ax + (\mu + \delta)c] + (\mu - \delta)c & \text{if } x^{(1)} \geq 0 \\ A[Bx + (\mu + \delta)c] + (\mu - \delta)c & \text{if } x^{(1)} \leq 0 \end{cases} . \quad (33)$$

**Lemma 3.1.** *F maps a neighborhood of  $y_{\text{lower}}(\mu, \delta)$  into itself and, with respect to an appropriate norm, is a contraction there.*

**Proof:** Given a nonsingular matrix  $S$ , we define the  $S$ -norm of a vector  $v$  as

$$\|v\|_S = \|Sv\| \quad (34)$$

and that of a matrix  $M$  as

$$\|M\|_S = \|S M S^{-1}\| . \quad (35)$$

For the matrix  $S$  in Condition 8, we have  $\theta = \max\{\|A^2\|_S, \|A B\|_S\} < 1$ .

To prove  $F$  in (33) is a contraction, we consider  $x$  and  $y$  in a neighborhood of  $y_{\text{lower}}$  and treat the following three cases separately.

1.)  $x^{(1)}, y^{(1)} \geq 0$ . It follows from (33) that

$$\|F(x) - F(y)\|_S = \|A^2(x - y)\|_S \leq \|A^2\|_S \|(x - y)\|_S \leq \theta \|x - y\|_S \quad (36)$$

2.)  $x^{(1)}, y^{(1)} \leq 0$ . It follows from (33) that

$$\|F(x) - F(y)\|_S = \|A B(x - y)\|_S \leq \|A B\|_S \|(x - y)\|_S \leq \theta \|x - y\|_S \quad (37)$$

3.)  $x^{(1)} \geq 0$  and  $y^{(1)} \leq 0$ . Let  $z$  be the point where the line between  $x$  and  $y$  intersects the plane  $\{z^{(1)} = 0\}$ . This choice of  $z$  implies that  $Az = Bz$  and  $\|x - z\|_S + \|z - y\|_S = \|x - y\|_S$ . It follows from (33) that

$$\|F(x) - F(y)\|_S = \|A^2 x - AB y\|_S = \|A^2(x - z) + AB(z - y)\|_S \quad (38)$$

$$\leq \|A^2\|_S \|x - z\|_S + \|AB\|_S \|y - z\|_S \quad (39)$$

$$\leq \theta \|x - z\|_S + \theta \|y - z\|_S = \theta \|x - y\|_S. \quad (40)$$

Moreover, since  $y_{\text{lower}}$  is a fixed point,  $F$  maps a neighborhood of  $y_{\text{lower}}$  into itself. ■

**Theorem 3.2.** *Condition 8 implies that the period-two orbit  $y_{\text{upper}}, y_{\text{lower}}$  is stable.*

**Proof:** For  $\mu > \mu_{\text{crit}}$  and  $\mu < \mu_{\text{crit}}$ , stability of the iterations is guaranteed because  $\forall i, |\lambda_i(A^2)| < 1$  and  $|\lambda_i(BA)| < 1$ , respectively. For  $\mu \approx \mu_{\text{crit}}$ , stability is guaranteed because  $F$  is a contraction, as shown in the proof of Lemma 3.1. ■

## 4 Prebifurcation gain

### 4.1 Analysis

Near the onset of a classical period-doubling bifurcation, disturbances in the bifurcation parameter may cause amplified disturbances in the system response, a phenomenon known as prebifurcation amplification. Various authors studied prebifurcation amplification for a classical period-doubling bifurcation, using a gain, which is the ratio of the response magnitude to the applied perturbation amplitude [16, 17, 18]. An analytical formula of the gain, including crucial higher-order terms, was derived in [19]. It is interesting to compute the gain for a B/C period-doubling bifurcation and compare with that of a classical period-doubling bifurcation. To this end, let us define a gain using the 1st component of the solution

$$\Gamma \equiv \frac{y_{\text{upper}}^{(1)} - y_{\text{lower}}^{(1)}}{2|\delta|}. \quad (41)$$

Then, the prebifurcation gain (when  $\mu \geq 0$ ) is described by the following theorem.

**Theorem 4.1.** *When  $\mu \geq 0$  and  $\delta \neq 0$ , the gain satisfies*

$$\Gamma = \begin{cases} \Gamma_{\text{const}}, & \text{if } \mu \geq \rho|\delta| \\ \Gamma_{\text{const}} + \gamma \left( \rho - \frac{\mu}{|\delta|} \right) & \text{if } \mu \leq \rho|\delta| \end{cases}, \quad (42)$$

where  $\Gamma_{\text{const}}$  and  $\gamma$  are positive constant, and  $\rho$  is given by (24).

**Proof:** When  $\mu \geq \rho|\delta|$ , the response to alternate pacing is an unilateral solution, as shown in the previous section. It follows from Equation (22) that

$$\Delta y = y_{\text{upper}} - y_{\text{lower}} = 2\delta d. \quad (43)$$

By the definition (41) and recalling the sign convention (21), the gain is

$$\Gamma = \left| d^{(1)} \right| \equiv \Gamma_{\text{const}}. \quad (44)$$



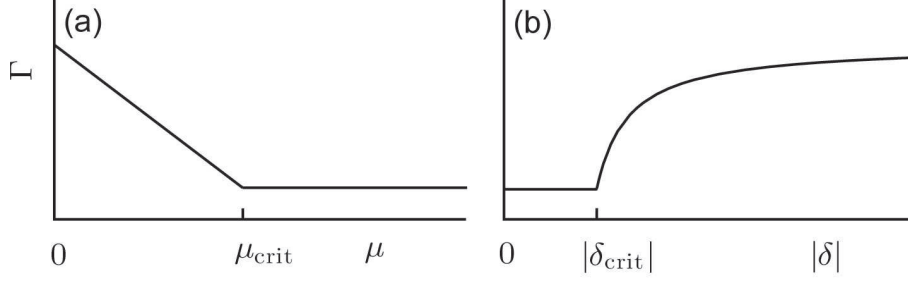


Figure 3: Schematic of the variation of the canonical gain (41) under changes in parameters: (a)  $\Gamma$  vs.  $\mu$  when  $\delta$  stays constant and (b)  $\Gamma$  vs.  $\delta$  when  $\mu$  stays constant.

Therefore, if  $\mu$  is varied and  $\delta$  is held fixed, the gain stays constant as long as  $\mu \geq \mu_{\text{crit}}(\delta) = \rho|\delta|$ , see Figure 3 (a). Similarly, if  $\delta$  is varied and  $\mu$  is held fixed, the gain stays constant as long as  $|\delta| \leq \delta_{\text{crit}}(\mu)$ , where  $\delta_{\text{crit}}(\mu) = \mu/\rho$ , see Figure 3 (b).

When  $\mu \leq \rho|\delta|$ , the response to alternate pacing is a bilateral solution, as shown in the previous section. It follows from Equations (31) and (32) that

$$\begin{aligned} \Delta y &= y_{\text{upper}} - y_{\text{lower}} \\ &= y_{\text{u-crit}} - y_{\text{l-crit}} + (\mu_{\text{crit}}(\delta) - \mu) (X_{\text{upper}} - X_{\text{lower}}) \\ &= 2\delta d + (\mu_{\text{crit}}(\delta) - \mu) (X_{\text{upper}} - X_{\text{lower}}), \end{aligned} \quad (45)$$

where we have used (25) and (26) for  $y_{\text{u-crit}}$  and  $y_{\text{l-crit}}$ . Recalling the definition (41) and using (44), the gain is

$$\Gamma = \Gamma_{\text{const}} + \gamma \left( \rho - \frac{\mu}{|\delta|} \right), \quad (46)$$

where

$$\gamma = \frac{1}{2} \left( X_{\text{upper}}^{(1)} - X_{\text{lower}}^{(1)} \right). \quad (47)$$

Here,  $\gamma > 0$ , since  $X_{\text{upper}}^{(1)} > 0$  and  $X_{\text{lower}}^{(1)} < 0$ . Therefore, for a constant  $\delta$ , the gain increases as  $\mu$  decreases from  $\mu_{\text{crit}} = \rho|\delta|$ , see Figure 3 (a). On the other hand, for a constant  $\mu$ , the gain increases as  $|\delta|$  increases from  $|\delta_{\text{crit}}| = \mu/\rho$ , see Figure 3 (b). ■

The precise relations (42), which hold for all  $\mu$  and  $\delta$ , result from the normal form (1), in which higher-order terms have been dropped. If such terms are present, then (42) will describe the qualitative behavior of the gain near the bifurcation point for small perturbation amplitude. In Section 4.2 we present a numerical example with the B/C period-doubling bifurcation in the cardiac model of Sun et al. [15]; this example shows that the leading-order analysis accurately capture the behavior of the model.

**Remark:** Analogous to  $\Gamma$ , a generalized gain can be defined using an arbitrary component of  $y$  as

$$g^{(i)} \equiv \frac{y_{\text{upper}}^{(i)} - y_{\text{lower}}^{(i)}}{2|\delta|}. \quad (48)$$

It follows from (43) and (45) that

$$g^{(i)} = \begin{cases} g_{\text{const}}^{(i)}, & \text{if } \mu \geq \rho |\delta| \\ g_{\text{const}}^{(i)} + \left(\rho - \frac{\mu}{|\delta|}\right) k^{(i)}, & \text{if } \mu \leq \rho |\delta| \end{cases}, \quad (49)$$

where

$$g_{\text{const}}^{(i)} = \left(\text{sign } d^{(1)}\right) d^{(i)}, \quad k^{(i)} = \frac{1}{2} \left(X_{\text{upper}}^{(i)} - X_{\text{lower}}^{(i)}\right). \quad (50)$$

As we saw above,  $g_{\text{const}}^{(1)} = \Gamma_{\text{const}} > 0$  and  $k^{(1)} = \gamma > 0$ . However, if  $i \neq 1$ , the signs of  $g_{\text{const}}^{(i)}$  and  $k^{(i)}$  are not uniquely determined. Thus, the generalized gain may have either sign and, even if positive, may exhibit monotonicity opposite to that in Figure 3. However, all gains are constant when  $\mu \geq \rho |\delta|$ .

## 4.2 A numerical example

Sun *et al.* [15] presented a theoretical model for atrioventricular nodal conduction, which accurately predicts a variety of experimentally observed cardiac rhythms. It was shown in [11] that the model of Sun *et al.* exhibits a border-collision period-doubling bifurcation. Following the notation of [11], the model iterates the atrial His interval,  $A$ , and the drift in the nodal conduction time,  $R$ , as follows

$$\begin{pmatrix} A_{n+1} \\ R_{n+1} \end{pmatrix} = \begin{cases} \begin{pmatrix} A_{\min} + R_{n+1} + (201 - 0.7A_n) e^{-H/\tau_{\text{rec}}} \\ R_n e^{-(A_n+H)/\tau_{\text{fat}}} + \gamma e^{-H/\tau_{\text{fat}}} \end{pmatrix}, & \text{if } A_n \leq 130 \\ \begin{pmatrix} A_{\min} + R_{n+1} + (500 - 3.0A_n) e^{-H/\tau_{\text{rec}}} \\ R_n e^{-(A_n+H)/\tau_{\text{fat}}} + \gamma e^{-H/\tau_{\text{fat}}} \end{pmatrix}, & \text{if } A_n \geq 130 \end{cases}, \quad (51)$$

where  $A_{\min} = 33$  ms,  $\tau_{\text{rec}} = 70$  ms,  $\tau_{\text{fat}} = 30\,000$  ms, and  $\gamma = 0.3$  ms. The bifurcation parameter,  $H$ , represents the time interval between bundle of His activation and the subsequent activation. Under variation of  $H$ , a border-collision period-doubling bifurcation occurs at  $H_{\text{bif}} = 56.9078$  ms, where of course  $A = 130$  at the bifurcation point. We apply alternate pacing to the above model by perturbing  $H$  with  $(-1)^k \delta$ . Figure 4 shows the relation between the gain  $\Gamma$  and the parameters  $H$  and  $\delta$ , computed from our theory as well as from numerical simulations. The agreement between the theoretical and the numerical results is good.

## 5 Summary and discussion

A border-collision (B/C) bifurcation occurs when the fixed point of an iterated map encounters a border on which the underlying map is continuous but its derivatives jump. Using the normal form (1), we presented the conditions for a B/C period-doubling bifurcation in multiple dimensional maps. Under these conditions, we computed the response of the map under a subharmonic perturbation to the bifurcation parameter, i.e. alternate pacing. The response under alternate pacing can be either unilateral or bilateral. As the names suggest, the two points of a unilateral solution lie on the same side of the border, while those of a bilateral solution lie on different sides of the border. The response to alternate pacing is quantified through the definition of a gain. We found

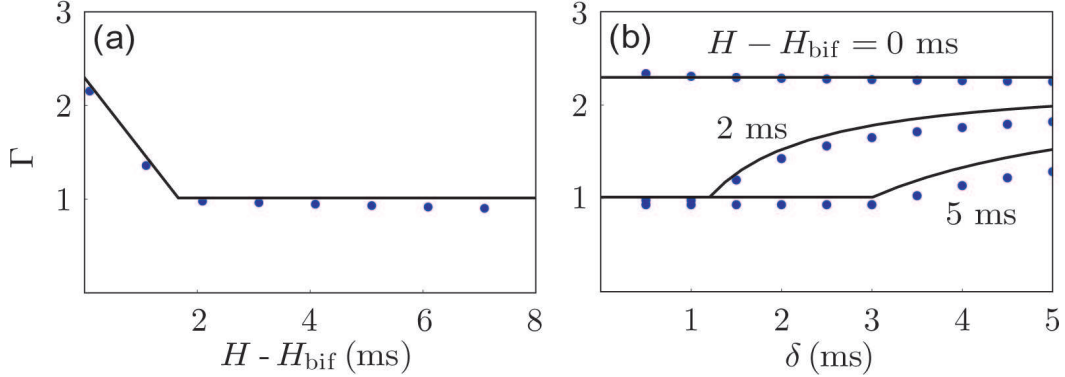


Figure 4: Alternate pacing of the model of Sun *et al.* (51): (a) variation of the gain  $\Gamma$  under changes of  $H$  when  $\delta = 1$  ms and (b) variation of the gain  $\Gamma$  under changes of  $\delta$  when  $H - H_{\text{bif}} = 0, 2,$  and  $5$  ms. Here, the solid curves indicate theoretical results and the dots indicate numerical simulations.

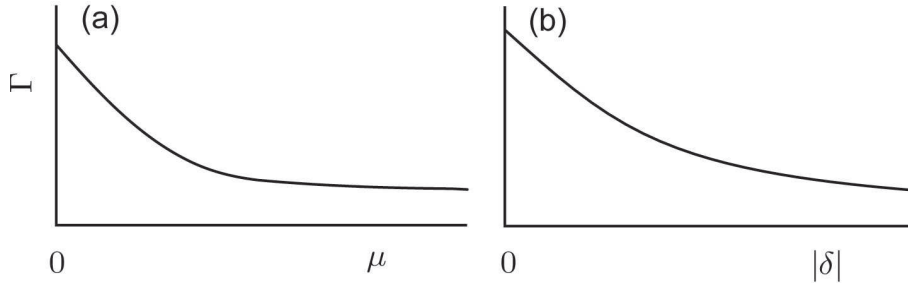


Figure 5: Schematic of the variation of the gain of a classical bifurcation under changes in parameters: (a)  $\Gamma$  vs.  $\mu$  when  $\delta$  stays constant and (b)  $\Gamma$  vs.  $\delta$  when  $\mu$  stays constant.

that the gain is a piecewise smooth function of the bifurcation parameter ( $\mu$ ) and the perturbation amplitude ( $|\delta|$ ), with qualitatively different behaviors in different parameter regions.

Most importantly, the gain in a border-collision bifurcation differs qualitatively from that in a classical bifurcation. For example, it follows from [19] that, after appropriate rescaling of the parameters, the gain of a classical period-doubling bifurcation satisfies the relation,

$$\delta^2 \Gamma^3 + \mu \Gamma - 1 = 0. \quad (52)$$

Figure 5 (a) and (b) schematically show the dependence of  $\Gamma$  on  $\mu$  and  $\Gamma$  on  $\delta$ , respectively. Comparison of (42) and (52) reveals two differences between the gain in a classical bifurcation and that in a border-collision bifurcation. (1) The gain of a classical bifurcation tends to infinity<sup>2</sup> as  $(\mu, \delta)$  approaches  $(0, 0)$ ; by contrast, the gain of a border-collision bifurcation is bound for all  $\delta \neq 0$ . (2) The gain of a classical bifurcation varies smoothly under changes in system parameters while that of a border-collision bifurcation undergoes a nonsmooth variation as parameters cross a boundary in the parameter space.

<sup>2</sup>Moreover, the rate of divergence as the parameters  $(\mu, \delta)$  tend to  $(0, 0)$  depends on the path taken. For example, when  $\delta$  is extremely small, the gain tends to infinity as  $\mu^{-1}$ ; on the other hand, when  $\mu = 0$ , the gain tends to infinity as  $\delta^{-2/3}$ .

Although the two cases exhibit these differences, if  $\Gamma$  is plotted as a function of  $\mu$  (with  $\delta$  held fixed), it may be difficult to distinguish them based on data from experiments, because only discrete points can be sampled and these are subject to experimental errors (cf. Figures 3 (a) and 5 (a)). However, if  $\Gamma$  is plotted as a function of  $\delta$  (with  $\mu$  held fixed), the distinction between the two bifurcation types is evident even with just a few data points and in the presence of experimental noise (cf. Figures 3 (b) and 5 (b)). Indeed, the theory in this paper guided the experiments [2] in identifying the type of a bifurcation in a paced cardiac tissue.

### Acknowledgments

Support of the National Institutes of Health under grant 1R01-HL-72831 and the National Science Foundation under grants DMS-9983320 and PHY-0243584 is gratefully acknowledged. The authors are also grateful to Carolyn Berger, Daniel J. Gauthier, and Wanda Krassowska for their insightful discussion.

## Appendix: The out-of-phase bilateral solution

Recall that, for the unilateral solution under alternate pacing,  $y_{\text{upper}}$  occurs for  $n$  odd due to the sign convention (21), and this behavior continues for the bilateral solution computed in Section 3.2; i.e. this bilateral solution is in phase with the unilateral solution. Thus, we refer to such bilateral solution as an *in-phase* bilateral solution. On the other hand, when  $\mu$  is sufficiently large negative, there exists a bilateral solution with the opposite phase; i.e.,  $y_{\text{upper}}$  occurs for  $n$  even. We refer to the latter as an *out-of-phase* bilateral solution.

Continuing the notation as in (27), the out-of-phase bilateral solution is characterized by the following equations

$$y_{\text{upper}} = B y_{\text{lower}} + (\mu - \delta) c, \quad y_{\text{lower}} = A y_{\text{upper}} + (\mu + \delta) c. \quad (53)$$

Note the signs of the terms  $\pm\delta c$  are different in the above equations and (28). Solving the above equations yields

$$y_{\text{upper}}(\mu, \delta) = x_{\text{upper}}(\mu) - \delta s_{\text{upper}}, \quad y_{\text{lower}}(\mu, \delta) = x_{\text{lower}}(\mu) + \delta s_{\text{lower}}, \quad (54)$$

where  $x_{\text{upper}}$  and  $x_{\text{lower}}$  have been computed in Equation (15), and the  $\mu$ -independent shifts  $s_{\text{upper}}$ ,  $s_{\text{lower}}$  have been computed in Equation (30). Note that the out-of-phase and in-phase bilateral solutions are parallel to each other because they are both parallel to the solution  $x_{\text{upper}}(\mu)$ ,  $x_{\text{lower}}(\mu)$ . One can show that the out-of-phase bilateral solution exists only when  $\mu X_{\text{upper}}^{(1)} \geq \delta s_{\text{upper}}^{(1)}$ . As required in Condition 6,  $X_{\text{upper}}^{(1)} < 0$ . Therefore,  $\mu$  has to be sufficiently large negative for the out-of-phase bilateral solution to exist.

## References

- [1] S. Banerjee and C. Grebogi, ‘Border collision bifurcations in two-dimensional piecewise smooth maps,’ Phys. Rev. E **59**, 4052, 1999.

- [2] C.M. Berger, X. Zhao, D.G. Schaeffer, W. Krassowska, H. Dobrovolny, and D.J. Gauthier, ‘Evidence for an unfolded border-collision bifurcation in paced cardiac tissue,’ submitted.
- [3] M. di Bernardo, M.I. Feigin, S.J. Hogan, and M.E. Homer, ‘Local analysis of C-bifurcation in n-Dimensional Piecewise-smooth dynamical systems,’ *Chaos, Solitons and Fractals*, **10**, 1881-1908, 1999.
- [4] M. di Bernardo, C. Budd, A. Champneys, and P. Kowalczyk, *Bifurcation and Chaos in Piecewise-smooth Dynamical Systems: Theory and Applications*, Springer-Verlag, in process.
- [5] M.I. Feigin, ‘Doubling of the Oscillation Period with C-Bifurcations in Piecewise Continuous Systems,’ *Prikl. Mat. Mekh.* **34**, 861-869, in Russian, 1970.
- [6] M.I. Feigin, ‘On the Generation of Sets of Subharmonic Modes in a Piecewise Continuous System,’ *Prikl. Mat. Mekh.* **38**, 810-818, in Russian, 1974.
- [7] M.I. Feigin, ‘On the Structure of C-Bifurcation Boundaries of Piecewise Continuous Systems,’ *Prikl. Mat. Mekh.* **42**, 820-829, in Russian, 1978.
- [8] M. Golubitsky and D.G. Schaeffer, *Singularities and Groups in Bifurcation Theory: Vol. I*, Applied Mathematical Sciences 51, Springer-Verlag, New York, 1985.
- [9] M.A. Hassouneh, ‘Feedback control of border collision bifurcations in piecewise smooth systems,’ Ph.D. dissertation, University of Maryland, College Park, Maryland, 2003.
- [10] M. A. Hassouneh, E. H. Abed, and H. E. Nusse, ‘Robust dangerous border-collision bifurcations in piecewise smooth systems,’ *Physical Review Letters*, **92**, 070201, 2004.
- [11] M.A. Hassouneh and E.H. Abed, ‘Border collision bifurcation control of cardiac alternans,’ *International J. of Bifurcations Chaos* **14**, 3303-3315, 2004.
- [12] A. Karma and Y. Shiferaw, ‘New Pacing Protocol for the Induction of T-wave alternans at Slower Heart Rate and Improving the Prediction of Sudden Cardiac Death,’ *NASPE Heart Rhythm Society 2004*, May 19 - 22, San Francisco, CA, 2004.
- [13] H.E. Nusse and J.A. Yorke, ‘Border-collision bifurcations including period two to period three for piecewise smooth systems,’ *Physica D* **57**, 39-57 1992.
- [14] H.E. Nusse, E. Ott, and J.A. Yorke, ‘Border-collision bifurcations: an explanation for observed bifurcation phenomena,’ *Physical Review E*, **49**, 1073-1076, 1994.
- [15] J. Sun, F. Amellal, L. Glass, and J. Billette, ‘Alternans and period-doubling bifurcations in atrioventricular nodal conduction,’ *J. Theor. Biol.* **173**, 79-91, 1995.
- [16] E. Surovyatkina, ‘Prebifurcation noise amplification and noise-dependent hysteresis as indicators of bifurcations in nonlinear geophysical systems,’ *Nonlinear Processes in Geophysics*, **12**, 25-29 (2005).
- [17] S.T. Vohra and K. Wiesenfeld, ‘Experimental Test of the Normal Form for Period Doubling Bifurcations,’ *Physica D* **86**, 27 (1995).

- [18] K. Wiesenfeld and B. McNamara, ‘Small-signal amplification in bifurcating dynamical systems,’ *Phys. Rev. A* **33**, 629 (1986); erratum: *ibid* **33**, 3578 (1986).
- [19] X. Zhao, D.G. Schaeffer, C.M. Berger, and D.J. Gauthier, ‘Small-Signal Amplification of Period-Doubling Bifurcations in Smooth Iterated Maps,’ *Nonlinear Dynamics*, to appear.
- [20] Z.T. Zhusubaliyev and E. Mosekilde, *Bifurcations and chaos in piecewise-smooth dynamical systems* (World Scientific, Singapore, 2003).